

Supporting Information

Non-monotonic first cycle irreversible capacity governed by delithiation depth in Li-rich layered cathodes

Liang Fang,^{a, ‡} Daseul Han,^{a, ‡} Seongkoo Kang,^b Un-Seon Heo,^a Kyung-Wan Nam^{*a} and Yong-Mook Kang^{*b,c}

^a*Department of Energy and Materials Engineering, Dongguk University-Seoul, Seoul 04620, Republic of Korea*

E-mail: knam@dongguk.edu

^b*Department of Materials Science and Engineering, Korea University, Seoul 02841, Republic of Korea*

E-mail: dake1234@korea.ac.kr

^c*KU-KIST Graduate School of Converging Science and Technology, Korea University, Seoul 02841, Republic of Korea*

[‡] *These authors contributed equally.*

^{*} Corresponded to K.-W. Nam (knam@dongguk.edu) and Y.-M. Kang (dake1234@korea.ac.kr)

Fig. S1-14, Tables S1-2.

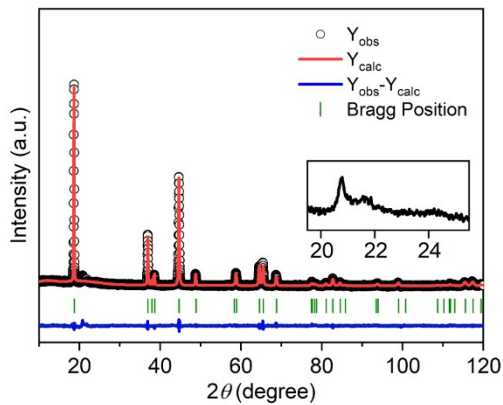


Fig. S1 XRD pattern and Rietveld refinement results of $\text{Li}_{1.2}\text{Ni}_{0.13}\text{Co}_{0.13}\text{Mn}_{0.54}\text{O}_2$.

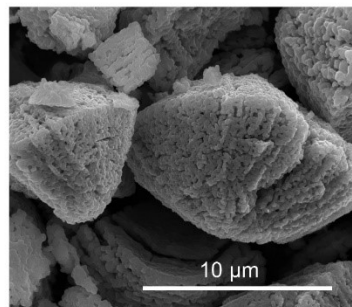


Fig. S2 SEM image of $\text{Li}_{1.2}\text{Ni}_{0.13}\text{Co}_{0.13}\text{Mn}_{0.54}\text{O}_2$.

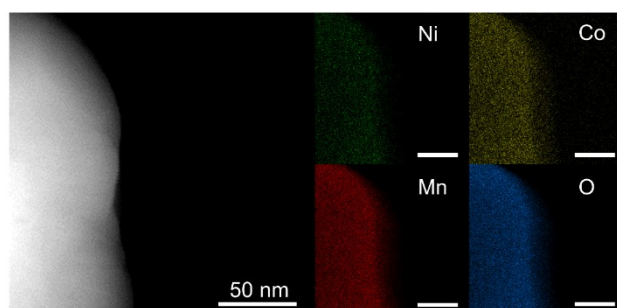


Fig. S3 EDS mapping results of $\text{Li}_{1.2}\text{Ni}_{0.13}\text{Co}_{0.13}\text{Mn}_{0.54}\text{O}_2$.

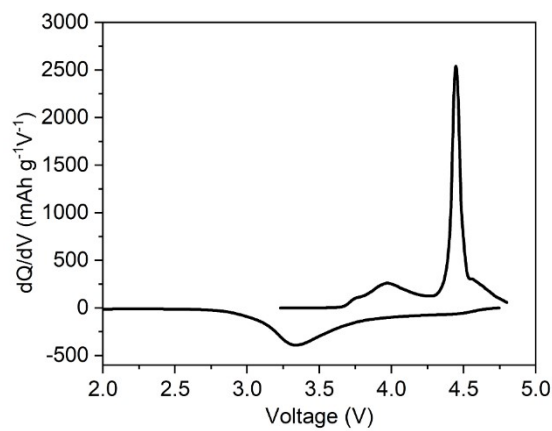


Fig. S4 dQ/dV curves of Fig. 1a.

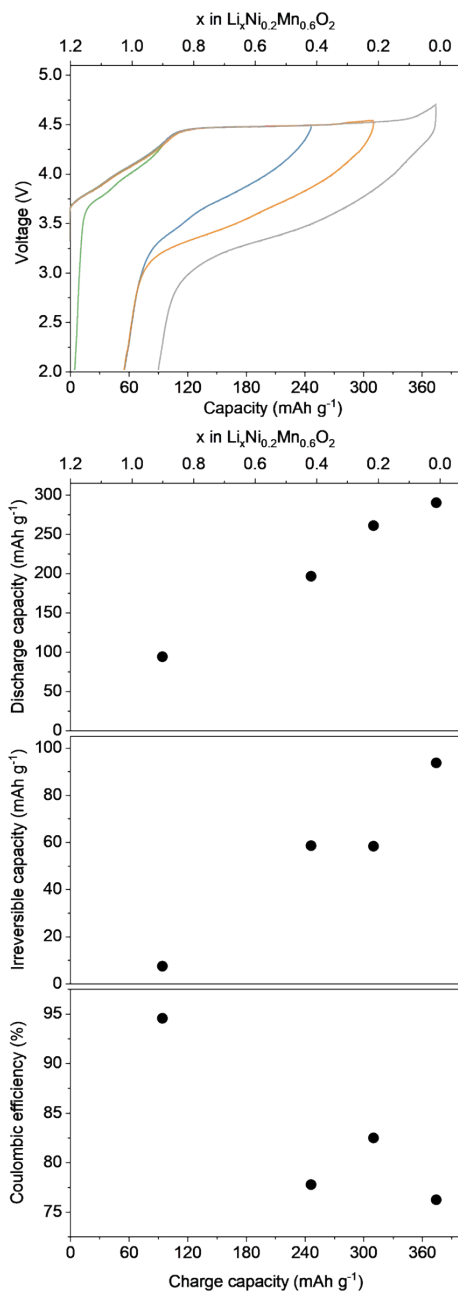


Fig. S5 (a) First-cycle electrochemical profiles with controlled charge capacity, (b) discharge capacity, irreversible capacity, and Coulombic efficiency in $\text{Li}_{1.2}\text{Ni}_{0.2}\text{Mn}_{0.6}\text{O}_2$ (i.e., 0.5Li₂MnO₃-0.5LiNi_{1/2}Mn_{1/2}O₂).

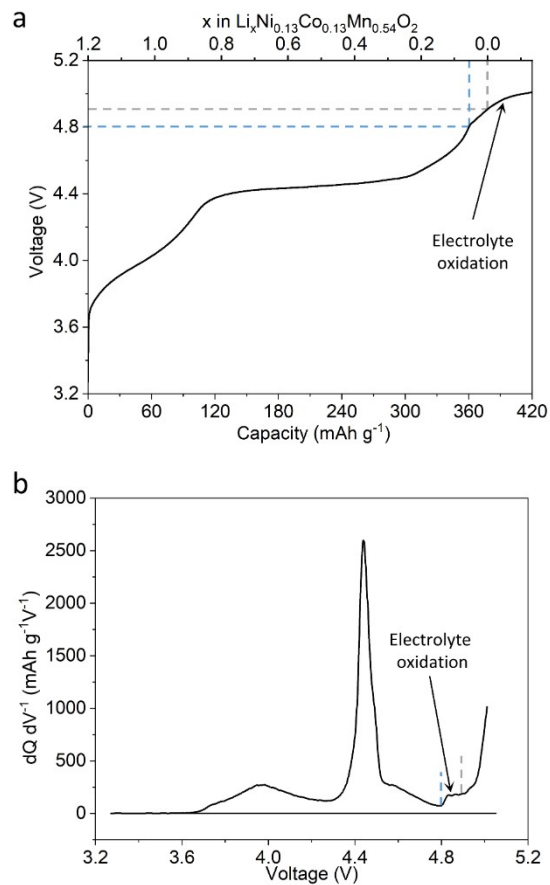


Fig. S6 (a) Charging profile for the first cycle to 420 mAh g⁻¹. (b) dQ/dV curves of (a).

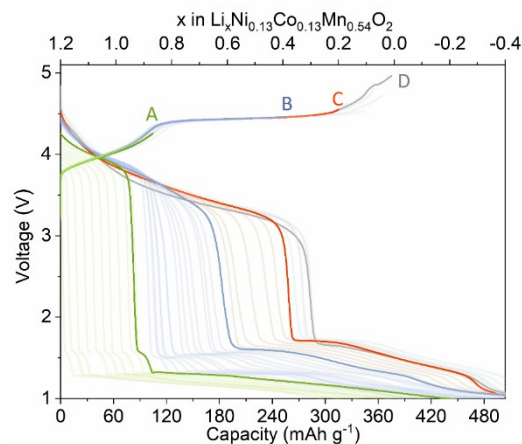


Fig. S7 First-cycle electrochemical profiles with controlled charge capacity from 5 to 395 mAh g⁻¹.

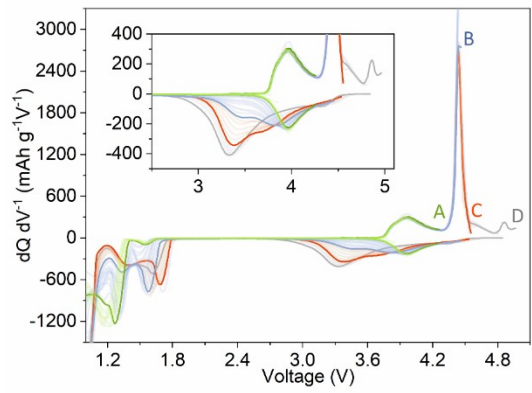


Fig. S8 dQ/dV curves of Fig. S5.

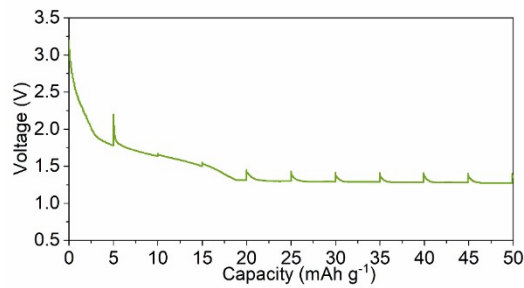


Fig. S9 GITT discharge profile of pristine material.

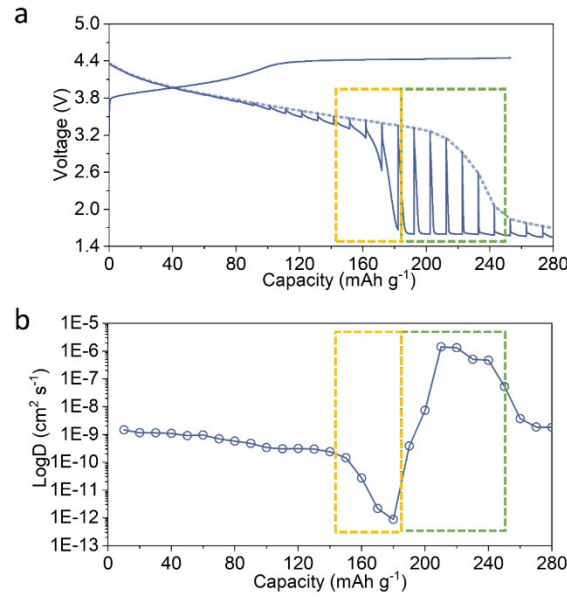


Fig. S10 (a) Capacity scaled GITT discharge profile after initial charge to 253 mAh g^{-1} . (b) Calculated lithium-ion diffusion coefficients of (a).

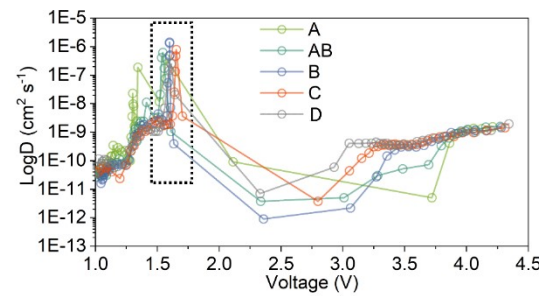


Fig. S11 Calculated lithium-ion diffusion coefficients of Fig. 2.

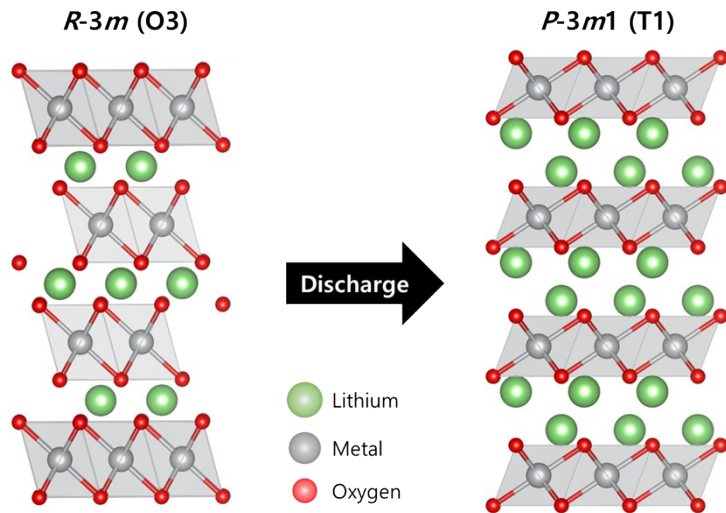


Fig. S12 Crystal structure of layered LiMO_2 (space group: $R-3m$) and overlithiated Li_2MO_2 (space group: $P-3m1$).

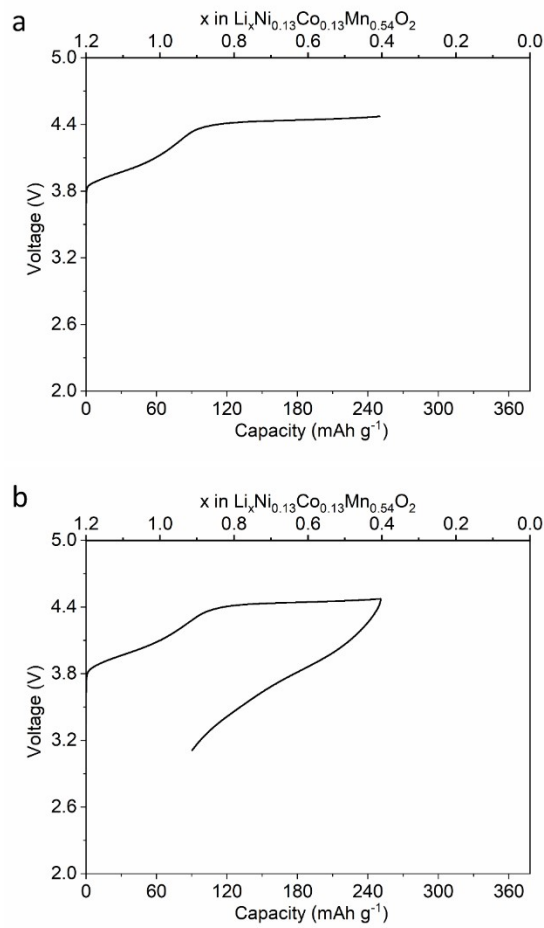


Fig. S13 The electrochemical profiles of pretreatment for operando synchrotron XRD. (a) to Fig. 3b and (b) to Fig. 3e.

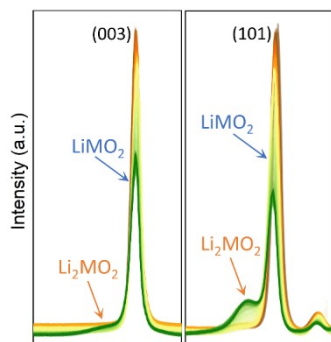


Fig. S14 The operando synchrotron XRD patterns of Fig. 3e in 1D.

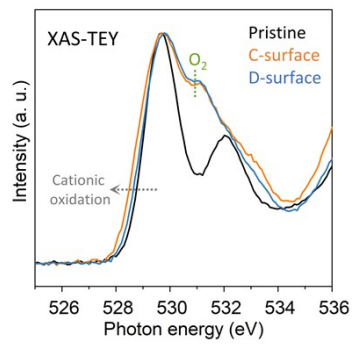


Fig. S15 O K-edge spectra measured in the TEY mode.

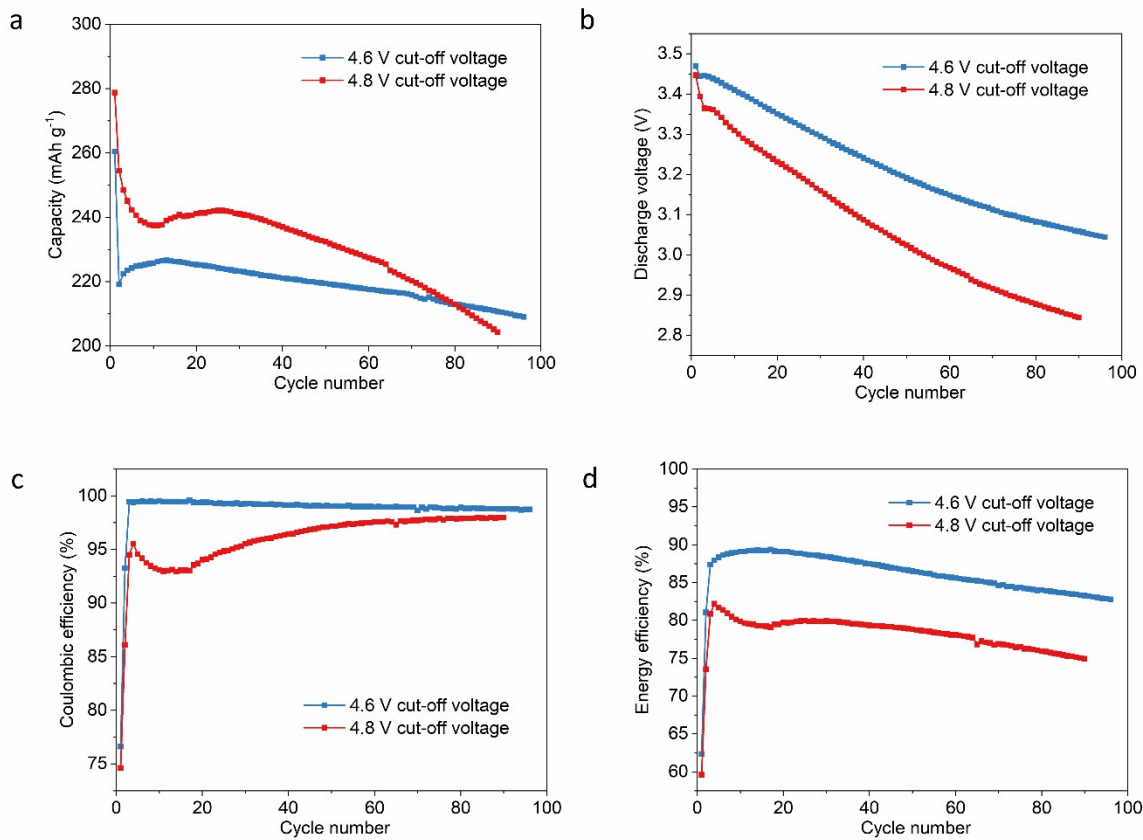


Fig. S16 (a) The capacity retention, (b) average discharge voltage, (c) coulombic efficiency, and (d) energy efficiency of $\text{Li}_{1.2}\text{Ni}_{0.13}\text{Co}_{0.13}\text{Mn}_{0.54}\text{O}_2$ cycled under 4.6 V and 4.8 V cut-off voltages.

Table S1 Rietveld refinement results of pristine $\text{Li}_{1.2}\text{Ni}_{0.13}\text{Co}_{0.13}\text{Mn}_{0.54}\text{O}_2$.

Crystal system	Rhombohedral					
Space group	R^3m (166)					
$a = 2.8466(3) \text{ \AA}$	$c = 14.218(2) \text{ \AA}$	Volume = 99.78(3)				
$\text{R}_{\text{wp}} = 1.95\%$	GOF = 1.21					
Atom	Site	x	y	z	Occ	B value
Li(1)	3b	0	0	0.5	1	0.25(3)
Li(2)/Ni(1)/Co(1)/Mn(1)	3a	0	0	0	0.2/0.13/0.13/0.54	0.25(3)
O1	6c	0	0	0.2586(1)	1	0.73(6)

theoretical chemical formula	measured atomic ratio			
	Li	Ni	Co	Mn
$\text{Li}_{1.2}\text{Ni}_{0.13}\text{Co}_{0.13}\text{Mn}_{0.54}\text{O}_2$	1.201(1)	0.134(1)	0.133(1)	0.534(1)

Table S2 Chemical composition analysis results from Inductively coupled plasma atomic emission spectroscopy (ICP-AES).